

# Solvent-Exposed Tryptophans Probe the Dynamics at Protein Surfaces

G. S. Lakshminikanth and G. Krishnamoorthy

Department of Chemical Sciences, Tata Institute of Fundamental Research, Mumbai 400 005, India

**ABSTRACT** The dynamics of single tryptophan (W) side chain of protease subtilisin *Carlsberg* (SC) and myelin basic protein (MBP) were used for probing the surface of these proteins. The W side chains are exposed to the solvent, as shown by the extent of quenching of their fluorescence by KI. Time-resolved fluorescence anisotropy measurements showed that the rotational motion of W is completely unhindered in the case of SC and partially hindered in the case of MBP. The rotational correlation time ( $\phi$ ) associated with the fast local motion of W did not scale linearly with the bulk solvent viscosity ( $\eta$ ) in glycerol-water mixtures. In contrast,  $\phi$  values of either W side chains in the denatured proteins or the free W scaled almost linearly with  $\eta$ , as expected by the Stokes-Einstein relationship. These results were interpreted as indicating specific partitioning of water at the surface of the proteins in glycerol-water mixtures.

## INTRODUCTION

The stability and function of globular proteins are expected to be controlled by their interaction with the solvent water. This expectation has led to a large number of investigations on the interaction of proteins with aqueous solvents (for comprehensive reviews see Gregory, 1995; Parsegian et al., 1995; Timasheff and Arakawa, 1996; Israelachvili and Wennerstrom, 1996; Bryant, 1996). The nature of interaction with the solvent could alter both the average structure and dynamics of various segments of proteins to various levels. Solvent-controlled flexibility and dynamics of protein enzymes have been correlated with their biological activity in some cases (Afleck et al., 1992; Broos et al., 1995). One would expect that the segments and side chains that are solvent-exposed to be controlled to a larger extent when compared to the interior region of the protein. However, there have been observations suggesting that the dynamics of even the interior regions are modulated by solvation (Afleck et al., 1992; Fitter et al., 1996; Priebe et al., 1996; Partridge et al., 1998).

Another consequence of the interaction of water with biological macromolecules is complementary in nature. The structure and dynamics of water near the surface of macromolecules differ from those of bulk water, as shown by x-ray crystallography (Teeter, 1991; Jiang and Brunger, 1994; Phillips and Pettitt, 1995; Burling et al., 1996), NMR studies (Brunne et al., 1993), molecular dynamics simulations (Teeter, 1991; Beveridge et al., 1993; Brunne et al., 1993; Knapp and Muegge, 1993; Billeter et al., 1996; Abseher et al., 1996; Makarov et al., 1998), and other theoretical studies (Nandi and Bagchi, 1997). The nature of the hydration shell around proteins has been of concern, especially with regard to the interaction of water with protein

surfaces. An ice-like ordered structure would be associated with density lower than that of bulk water. However, molecular dynamics simulations (Levitt and Sharon, 1988), crystallographic studies (Badger, 1993; Burling et al., 1996), and recent x-ray and neutron scattering studies (Svergun et al., 1998) have shown that the density of the hydration shell is significantly ( $\sim 10\%$ ) higher than that of bulk water. Hence any description of the nature of protein-water interaction should be able to explain the increased density. Apart from such structural information, knowledge of the dynamics of water at the interface would also be useful. Reduced rates of translational diffusion of water near the interface inferred from molecular dynamics simulations (Abseher et al., 1996; Makarov et al., 1998) is in line with water bound to macromolecular surfaces. Water structure around protein surfaces is expected to control processes such as protein folding and ligand binding, apart from imparting structural stability.

Rotational dynamics of protein side chains could be thought of as probes for inferring the dynamics of water near protein surfaces. Rotational relaxation of spin probes has been used to characterize the hydration-dependent dynamics of the lysozyme surface (Rupley et al., 1983). In the present work we have used time-dependent depolarization of fluorescence of tryptophan side chains located on protein surfaces to observe the behavior of water near protein surfaces. Our results suggest the presence of water bound to protein surfaces in their native states and not in their denatured states.

## MATERIALS AND METHODS

Steady-state fluorescence measurements were performed by using a SPEX (Edison, NJ) Fluorolog FL1T11 T-format fluorimeter. Time-resolved fluorescence intensity and anisotropy measurements were carried out by using either the picosecond laser-time-correlated single photon counting set-up described earlier (Swaminathan et al., 1994b, 1996) or a Ti-sapphire femto/picosecond laser (Spectra Physics, Mountain View, CA) pumped by a Nd-YLF laser (Millennia X; Spectra Physics). In the latter case, 1-ps pulses of 885-nm radiation from the Ti-sapphire laser were frequency tripled to 295 nm by using a frequency doubler/tripler (GWU; Spectra Physics).

Received for publication 16 January 1999 and in final form 14 May 1999.

Address reprint requests to Dr. G. Krishnamoorthy, Department of Chemical Sciences, Tata Institute of Fundamental Research, Homi Bhabha Road, Mumbai 400 005, India. Tel.: 91-22-215-2971, ext. 2979; Fax: 91-22-215-2110 or 2181; E-mail: gk@tiffr.res.in.

© 1999 by the Biophysical Society

0006-3495/99/08/1100/07 \$2.00

The proteins subtilisin *Carlsberg* (SC) and myelin basic protein (MBP) were purchased from Sigma Chemical Co (St. Louis, MO). The purity of the proteins was checked by sodium dodecyl sulfate-polyacrylamide gel electrophoresis. Coomassie blue stains showed essentially a single band for the two proteins. The native and denatured protein solutions were prepared in 20 mM phosphate pH 7.0 buffer and 6 M guanidine hydrochloride (GdnHCl) in 20 mM phosphate pH 7.0 and equilibrated at 25°C for several hours. The concentrations of the proteins and L-tryptophan were in the range of 20–200  $\mu$ M. The bulk viscosity was increased by adding ultrapure glycerol. Viscosity was measured with an Ostwald's viscometer. Fresh solutions of the fluorescence quencher KI contained 100  $\mu$ M sodium thiosulfate to inhibit the formation of  $I_3^-$  ions. All of the measurements were carried out at  $\sim 25^\circ\text{C}$ .

The protein and L-tryptophan samples were excited by 295-nm pulses at 800 kHz, and the fluorescence collected at 360 nm was analyzed by the time-correlated single photon counting set-up. Fluorescence intensity decays were deconvoluted with the instrument response function and analyzed as a sum of exponentials:

$$I(t) = \sum \alpha_i \exp(-t/\tau_i) \quad (1)$$

where  $I(t)$  is the fluorescence intensity at time  $t$  and  $\alpha_i$  is the amplitude of the  $i$ th lifetime  $\tau_i$  such that  $\sum_i \alpha_i = 1$ .

Time-resolved anisotropy decays were analyzed by the following equations:

$$I_{\parallel}(t) = I(t)[1 + 2r(t)]/3 \quad (2)$$

$$I_{\perp}(t) = I(t)[1 - r(t)]/3 \quad (3)$$

$$r(t) = r_0\{\beta_1 \exp(-t/\phi_1) + \beta_2 \exp(-t/\phi_2)\} \quad (4)$$

where  $I_{\parallel}$  and  $I_{\perp}$  are the emission intensities collected at polarizations parallel and perpendicular, respectively, to the polarization of the excitation light.  $r(t)$  is the anisotropy at time  $t$ ,  $r_0$  is the initial anisotropy, and  $\phi$ 's are the rotational correlation times. The signal-to-noise ratio of our experiments was not sufficient to recover more than two correlation times. In the case of SC,  $\phi_1$  had  $>90\%$  amplitude, and hence it could be estimated with  $<10\%$  uncertainty. However, in the case of MBP,  $\phi_1$  and  $\phi_2$  had nearly equal amplitudes, and hence their estimation was nontrivial. An initial estimate of all parameters was obtained by floating all the parameters. Subsequently  $\phi_1$  was fixed at a value, and the other parameters floated. In this way a surface of  $\chi^2$  versus  $\phi_1$  was generated. The pattern of distribution of residuals was also carefully scrutinized at each trial. It was noted that the residual distribution pattern was a better diagnosis when compared to the  $\chi^2$  criterion for selecting the best value of  $\phi_1$ . The uncertainty in the value of  $\phi_1$  (in MBP) estimated in this way varied from  $\sim 20\%$  at 0% glycerol and  $\sim 15\%$  at 40% glycerol. Furthermore, the near constancy of the ratio  $\beta_1/\beta_2$  at all concentrations of glycerol also supports the estimates of  $\phi_1$  and  $\phi_2$ .

Rotational dynamics of macromolecule-attached fluorophores are generally described by the model in which the fluorophore has at least two types of motions, viz., global rotation of the entire macromolecule characterized by a rotational correlation time  $\phi_p$  and either free rotation of the fluorophore or segmental mobility of the region around the fluorophore collectively characterized by a rotational correlation time  $\phi_F$ . Assumption of independence between these two correlation times gives the following expression for the decay of  $r(t)$  (Lakowicz, 1983):

$$r(t) = r_0 [a \exp(-t/\phi_F) + (1 - a) \exp(-t/\phi_p)] \quad (5)$$

Comparison of Eqs. 4 and 5 gives  $\phi_p = \phi_2$  and  $\phi_F = \phi_1 \phi_p / (\phi_p - \phi_1)$ .  $\phi_F \approx \phi_1$  when  $\phi_F \ll \phi_p$ .

## RESULTS AND DISCUSSION

### The tryptophan side chains are solvent-exposed

One of the ideal ways of probing protein surfaces is to use solvent-exposed side chains. The single tryptophan side

chain of the protease subtilisin *Carlsberg* (SC) and myelin basic protein (MBP) are examples of solvent-exposed tryptophans (see Fig. 1 for the crystal structure of SC). Fig. 2 shows the fluorescence emission spectra of SC and MBP in their native and denatured states. The emission spectra of the model compound *N*-acetyl tryptophanamide (NATA) is also given for comparison. A fluorescence emission maximum of 355 nm observed for these tryptophans in both the native and denatured states and their similarity to the spectra of NATA indicate their solvent-exposed character in solutions. Furthermore, their solvent accessibility was checked by dynamic quenching of fluorescence by potassium iodide. Fig. 3 shows Stern-Volmer plots for the quenching of the fluorescence lifetime of both SC and MBP by iodide in both native and denatured states. (Fluorescence lifetimes were measured by pulse fluorimetry with a time resolution of 20 ps. The fluorescence decays were fitted to a sum of three or four exponentials. Similar multiexponential decays have been observed for several single tryptophan proteins (e.g., Swaminathan et al., 1994a).) It can be seen that the bimolecular quenching constant  $k_q$  obtained from these data (see the legend to Fig. 3) is very close to diffusion-controlled rates ( $10^9$ – $10^{10}$   $\text{M}^{-1} \text{ s}^{-1}$ ; Noyes, 1961). Furthermore, the values of  $k_q$  did not increase significantly when the proteins were denatured by guanidine hydrochloride (see the legend to Fig. 3). Accessibility to iodide is generally taken as an effective indication of exposure of a protein side chain to solvent (Eftink, 1991). The slight decrease in  $k_q$  seen in the denatured proteins when compared to the value in their native states could be explained as follows. In their native states the tryptophan side chains are solvent exposed, and approach to their location is unhindered by the compact

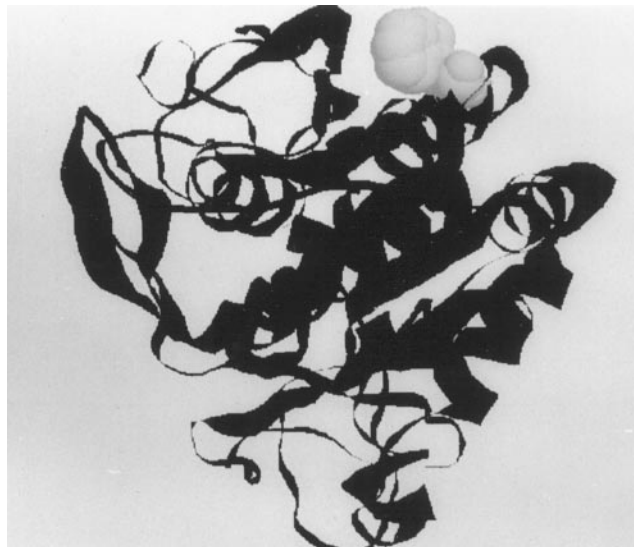


FIGURE 1 Crystal structure of subtilisin *Carlsberg* (SC). Rasmol software (Sayle and Milner-White, 1995) was used in constructing the structure from the coordinates taken from the Protein Data Bank. The single tryptophan side chain (represented by space-filling model) could be seen to be exposed to the solvent.

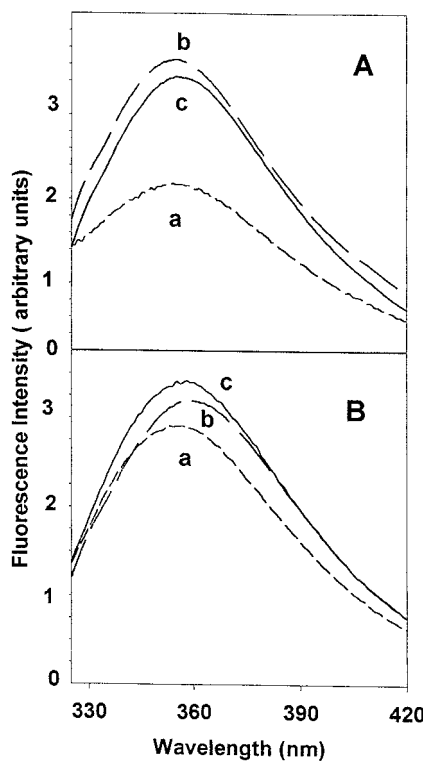


FIGURE 2 Fluorescence emission spectra of SC (A) and MBP (B) in their native (curves *a*) and denatured (curves *b*) states. The emission spectra of the model compound *N*-acetyl tryptophanamide (NATA) (curves *c*) is also given for comparison. The excitation was at 295 nm.

protein. In contrast, when the protein is denatured the access to the tryptophan side chain could be partially hindered by the nearby free-moving peptide chain. Taken together, these results clearly indicate that the tryptophan side chains of both of the proteins are exposed to the solvent.

### Rotational dynamics of the tryptophans

The rotational diffusion of the single tryptophan side chains in SC and MBP was determined from their rate of decay of fluorescence anisotropy. Typical curves of decay of fluorescence anisotropy are shown in Fig. 4. It can be seen that the decay rates are quite fast in both proteins. Analyses of the decay curves (see Materials and Methods) show the presence of at least two rotational correlation times ( $\phi$ ). The values of  $\phi$  were  $\sim 0.2$  ns ( $\sim 95\%$ ) and 3 ns ( $\sim 5\%$ ) in the case of SC and  $\sim 0.4$  ns ( $\sim 50\%$ ) and 2 ns ( $\sim 50\%$ ) in the case of MBP (Table 1). These values correspond to the native proteins in the absence of glycerol (see later). Similar results have been obtained by other workers (Janot et al., 1991; Maity, 1997). The longer  $\phi$  values (2–5 ns) could originate from either tumbling motion of the entire protein or the segmental mobility of a part of the protein. The shorter component (0.2–0.4 ns) could represent the rotational motion of the indole group with respect to the protein. In the case of SC, the observed value of  $\sim 0.2$  ns with  $\sim 90\%$  amplitude indicates that the rotational freedom of indole is

largely unrestricted. The smaller amplitude ( $\sim 50\%$ ) of the faster component observed in the case of MBP indicates partially restricted rotation of the indole moiety. This information, when coupled with the solvent accessibility assessed by iodide quenching (Fig. 3), indicates that the tryptophan side chains in both proteins would be capable of probing the dynamics of water at the surface of these proteins.

The rotational dynamics of the solvent-exposed tryptophan side chains in SC and MBP deserves further comment. The large amplitudes (95% in SC and 50% in MBP) associated with the faster component of depolarization (which represents the rotational dynamics of tryptophan with respect to the protein) would enable us to accurately probe the dynamics of water at the protein surface. We had observed that in a large number of proteins the global motion of the protein largely dominates the rotational dynamics of solvent-exposed side chains. In other words, solvent exposure alone does not ensure free rotation with respect to the protein. The present observation of large-amplitude fast motion of tryptophan in SC and MBP is rather fortuitous. Alternatively, one could think of covalently labeled extrinsic probes as having large-amplitude local dynamics. However, most of the commonly used fluorescence probes extend far from the surface, and hence they are unlikely to probe the dynamics of the water at the surface (see later). Furthermore, they could perturb the local structure and hence they are less likely to convey the dynamics of native structures.

### Effect of glycerol on the dynamics of surface tryptophans

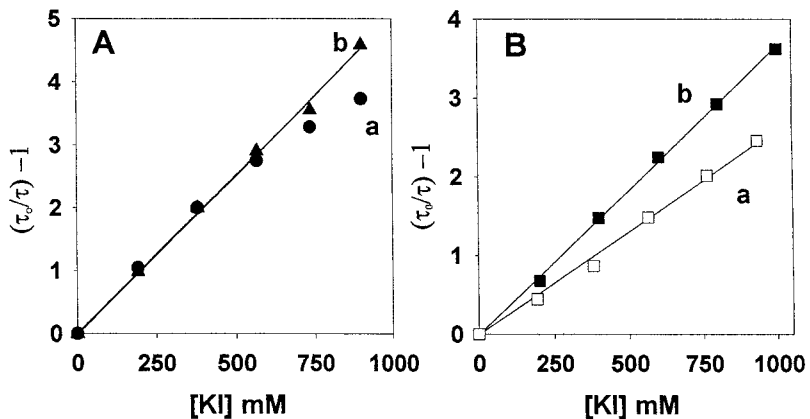
Formation of an ordered water structure on protein surfaces would imply preferential binding of water in the presence of a cosolvent. Binding of water is generally observed from x-ray crystallographic studies (Teeter, 1991; Badger, 1993; Burling et al., 1996; Jiang and Brunger, 1994; Phillips and Pettitt, 1995), NMR measurements (Brunne et al., 1993; Bryant, 1996), and thermodynamic estimations (Timasheff and Arakawa, 1996). Rotational dynamics of surface probes could be a novel way of inferring preferential binding of water. This could be achieved by monitoring the change in the rotational dynamics of the probes by the presence of a cosolvent such as glycerol. The bulk viscosity of solutions increases with the increase in the proportion of glycerol in glycerol-water mixtures. Rotational correlation times of small molecules (mol. wt.  $< 500$ ) vary linearly with the bulk viscosity in glycerol-water mixtures, as demanded by the Stokes-Einstein relationship for a spherical rotor,

$$\phi = \eta V / kT \quad (6)$$

where  $\eta$  is the viscosity and  $V$  is the molecular volume. To check whether  $\phi$  scales linearly with  $\eta$ , the following modified form of Eq. 6 was used:

$$\phi / \phi_0 = \eta / \eta_0 \quad (7)$$

FIGURE 3 Quenching of fluorescence of the tryptophan side chains of SC (A) and MBP (B) by KI in their native (curves a) and denatured (curves b) states.  $\tau_0$  and  $\tau$  are the mean fluorescence lifetimes ( $= \sum_i \alpha_i \tau_i$ ) in the absence and in the presence of KI, respectively. The bimolecular quenching constant  $k_q$  calculated by using the Stern-Volmer equation ( $\tau_0/\tau = 1 + k_q \tau_0 [KI]$ ) is  $5.3 \times 10^9 \text{ M}^{-1} \text{ s}^{-1}$  and  $2.0 \times 10^9 \text{ M}^{-1} \text{ s}^{-1}$  for native and denatured SC, respectively, and  $1.74 \times 10^9 \text{ M}^{-1} \text{ s}^{-1}$  and  $1.24 \times 10^9 \text{ M}^{-1} \text{ s}^{-1}$  for native and denatured MBP, respectively.



where  $\phi$  and  $\phi_0$  are the rotational correlation times at viscosity values  $\eta$  and  $\eta_0$ , respectively.  $\eta_0$  could correspond to some reference medium such as 0% glycerol. It is worth mentioning that evaluation of viscosity dependence of  $\phi$  by Eq. 7 does not require information on the effective rotational volume  $V$ . A slope of unity arising from a plot of  $\phi/\phi_0$  versus  $\eta/\eta_0$  would indicate a perfect scaling  $\phi$  with  $\eta$  according to Eq. 6. Any value of the slope of less than unity would be an indication of protection of the dipole from the bulk solvent.

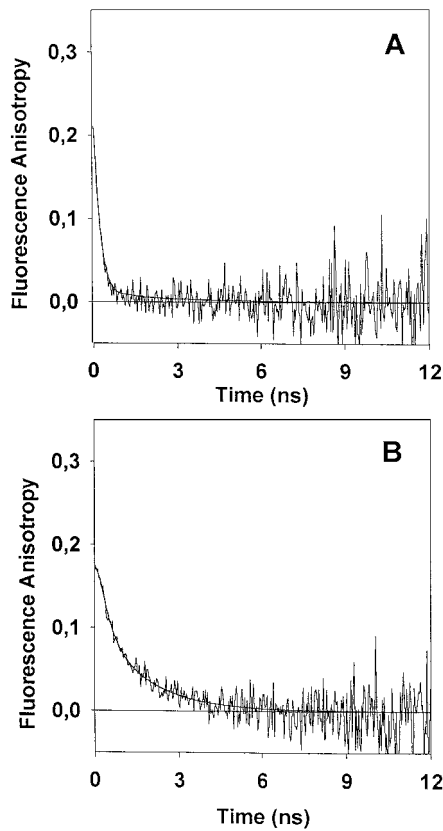


FIGURE 4 Typical decays of fluorescence anisotropy of SC (A) and MBP (B). The excitation and emission wavelengths were 295 nm and 360 nm, respectively. The smooth lines were calculated by the model given in Eqs. 2–4 and the parameters given in Table 1.

Fig. 5 shows the plots of the data given in Table 1 according to Eq. 7. The first observation from Fig. 5 is the unit slope in the case of free L-tryptophan, as expected from Eq. 6. In contrast, the tryptophan side chain on the surface of native SC showed a different picture. In this case,  $\phi_F$  did not scale linearly with  $\eta$ , as shown by the slope value of 0.23. This behavior was seen in the case of MBP, also through  $\phi_F$ , which represents the rotational mobility of the tryptophan with respect to the protein (Table 1 and Fig. 5). The slope was 0.16 in this case. This subscaling behavior of  $\phi_F$  with respect to  $\eta$  would indicate that the surface probes do not sense the bulk viscosity as faithfully as free probes in glycerol-water mixtures. This could be due to the presence of preferentially bound water, which ensures that the rotational dynamics of surface residues are dominantly controlled by bound water rather than by the more viscous glycerol-water mixture. The structural stability of the proteins in glycerol-water mixtures was monitored by circular dichroism (CD) spectra in the wavelength range of 210–250 nm (data not shown). No significant changes in the CD spectra were observed up to 50% glycerol (w/w). (In the case of MBP the estimated value of  $\phi_1$  has an error of 15–20% due to nearly equal amplitudes associated with  $\phi_1$  and  $\phi_2$  (see Materials and Methods). Hence the slope of  $\phi/\phi_0$  versus  $\eta/\eta_0$  plots will be in the range of 0.13–0.31. However, this variation does not alter our basic conclusions.)

In the case of MBP the longer correlation time ( $\phi_p$ ) of 2.3 ns had 50% amplitude, and hence it could be estimated with a good level of accuracy (unlike in the case of SC). As mentioned earlier, this component could have contributions from both global as well as segmental mobility. The dependence of  $\phi_p$  on bulk viscosity was significantly different from that of  $\phi_F$ . The plot of  $\phi_p$  according to Eq. 7 gave a slope of 0.54, which is significantly higher than that observed for  $\phi_F$ . This is in line with the contention that the longer  $\phi_p$  originates from global tumbling and segmental mobility, which are controlled by bulk viscosity.

To check whether the sublinear variation of  $\phi_F$  with  $\eta$  is a consequence of the native structure of the proteins or the covalently bound nature of the probe, measurements were carried out when the proteins were denatured by 6M GdnHCl. (In separate experiments it was confirmed (data

**TABLE 1** Fluorescence anisotropy decay parameters

System	$\eta/\eta_0$	Rotational correlation times (ns)*		Amplitudes		Initial anisotropy $r_0$	$\chi^2$
		$\phi_1$	$\phi_2$	$\beta_1$	$\beta_2$		
<b>L-Tryptophan</b>							
0% Glycerol	1.00	0.06				0.20	1.20
10% Glycerol	1.29	0.08				0.20	1.04
20% Glycerol	1.90	0.10				0.20	1.06
30% Glycerol	2.45	0.15				0.20	1.04
40% Glycerol	3.64	0.19				0.20	1.18
50% Glycerol	6.18	0.27				0.20	1.08
<b>Native SC</b>							
0% Glycerol	1.00	0.17	3.50	0.90	0.10	0.21	1.14
10% Glycerol	1.29	0.22	4.67	0.95	0.05	0.23	1.05
20% Glycerol	1.90	0.23	5.10	0.95	0.05	0.23	1.14
30% Glycerol	2.45	0.25	5.30	0.95	0.05	0.27	1.06
40% Glycerol	3.64	0.27	5.00	0.95	0.05	0.24	1.05
50% Glycerol	6.18	0.35	5.38	0.95	0.05	0.24	1.02
<b>Denatured SC</b>							
0% Glycerol	1.23	0.17	0.91	0.68	0.32	0.21	1.16
10% Glycerol	1.70	0.32	0.91	0.68	0.32	0.21	1.12
20% Glycerol	2.14	0.40	1.40	0.70	0.30	0.21	1.15
30% Glycerol	4.84	0.53	2.11	0.53	0.47	0.21	1.19
40% Glycerol	5.65	0.90	3.37	0.85	0.15	0.22	1.11
50% Glycerol	10.64	1.22	4.00	0.70	0.30	0.23	1.18
<b>Native MBP</b>							
0% Glycerol	1.00	0.44	2.30	0.50	0.50	0.18	1.05
10% Glycerol	1.29	0.44	2.80	0.50	0.50	0.19	1.00
20% Glycerol	1.90	0.47	3.30	0.45	0.55	0.18	1.07
30% Glycerol	2.45	0.70	3.80	0.40	0.60	0.18	1.04
40% Glycerol	3.64	0.73	5.00	0.40	0.60	0.18	1.09
50% Glycerol	6.18	0.87	9.09	0.40	0.60	0.19	1.12
<b>Denatured MBP</b>							
0% Glycerol	1.23	0.35	2.00	0.60	0.40	0.21	1.15
10% Glycerol	1.70	0.45	2.50	0.60	0.40	0.20	1.05
20% Glycerol	2.14	0.73	3.50	0.60	0.40	0.19	1.00
30% Glycerol	4.84	1.00	6.00	0.60	0.40	0.19	1.10
40% Glycerol	5.65	1.60	12.00	0.60	0.40	0.21	1.12

\*The error in the estimation of  $\phi_1$  was less than 10% in the cases of L-tryptophan and native SC and ~20% in other cases.  $\phi_2$  values have an uncertainty of ~25% in the case of native SC (due to the small amplitude of  $\beta_2 \approx 0.05$ ) and ~10–20% in other cases. For the estimation of these errors see Materials and Methods.

not shown) that the native to denatured state transition occurs well below 6 M GdnHCl for both proteins.) The data given in Table 1 and Fig. 5 show clearly that upon denaturation the extent of variation  $\phi_F$  with viscosity is significantly higher when compared to the native proteins. This was indicated by the increase in the slope to 0.98 and 0.82 in the case of SC and MBP, respectively (Fig. 5). This observation indicates that the lack of scaling of  $\phi_F$  with  $\eta$  (in the absence of GdnHCl) is mainly the consequence of the native structure of the proteins. However, in the case of denatured proteins, the extent of variation of  $\phi_F$  with  $\eta$  was still less than that observed with free tryptophan (slope = 0.94). The covalent attachment of the probe to the polypeptide could have resulted in a situation wherein the motional dynamics of the probe is dictated by the segmental motion of the polypeptide, also apart from the solvent viscosity.

### Characteristics of the protein-water interface

The experimental results described above clearly demonstrate the special nature of the interface in native proteins. This special nature lies in the ability of surfaces of native proteins to preferentially bind water in the presence of a cosolvent such as glycerol. The bound water could form a hydrogen-bonded network around the native protein. This network of bound water ensures that the dynamics of protein side chains are controlled by it and largely insulated from the bulk solvent. Such a protective coating is disrupted when the proteins are denatured. The lack of compact structure would not allow the formation of a stable hydrogen-bonded network of water. This leads to the situation where the side chain dynamics are controlled by the bulk solvent, also apart from the segmental motion of the polypeptide. It

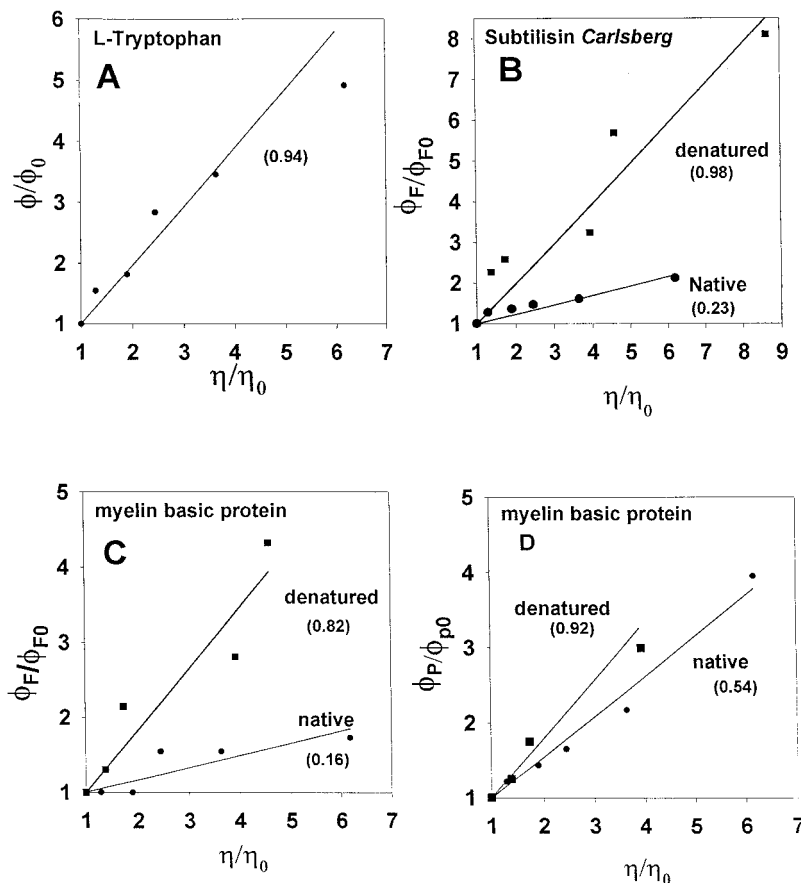


FIGURE 5. Plots of  $\phi/\phi_0$  versus  $\eta/\eta_0$  (Eq. 7), where the subscript 0 refers to 0% glycerol. (A) L-Tryptophan. (B) Native and denatured SC. (C and D) Native and denatured MBP. *B* and *C* correspond to  $\phi_F$ , and *D* corresponds to  $\phi_P$ . The slope is given near each plot (in parentheses).

is interesting to note that breakage of water structure by denaturants such as urea and GdnHCl has been implicated as a mechanism of protein denaturation (Vanzi et al., 1998). Furthermore, increased hydration of folded proteins when compared to denatured proteins has also been observed recently in the gas phase (Fye et al., 1998).

Although structured and bound water at protein surfaces has been inferred from a large number of techniques (Teter, 1991; Brunne et al., 1993; Beveridge et al., 1993; Knapp and Muegge, 1993; Jiang and Brunger, 1994; Phillips and Pettitt, 1995; Billeter et al., 1996; Nandi and Bagchi, 1997; Makarov et al., 1998; Fye et al., 1998), preferential binding of water in the presence of a cosolvent has been difficult to observe. Hence the present method of monitoring it through the dynamics of exposed side chains could prove to be useful.

Apart from indicating the presence of bound water at the surfaces, the present technique would also be useful in studying dynamics at the interfaces. Comparison of the  $\phi$  value of free tryptophan (in the absence of glycerol, 60 ps) with the faster  $\phi_F$  of tryptophan in SC (180 ps) suggests that the reduced rate of rotational motion of the indole moiety in proteins may be the result of either the presence of ordered water structure or the covalent attachment. A comparison of the  $\phi_F$  values in native and denatured SC in the absence of glycerol could be used to resolve this issue. The values of  $\phi_F$  were 0.18 ns and 0.22 ns for the native and denatured

SC, respectively. The latter value, when normalized to the viscosity of water (the viscosity of 6 M guanidine hydrochloride, which was used to denature the protein, is 1.2 cP), is 0.18 ns. Thus the higher value of  $\phi_F$  of 0.18 ns in the denatured state when compared to the value of 60 ps for the  $\phi_F$  of free tryptophan favors the second possibility, viz., damping of the rotational dynamics by covalent attachment. One could argue that because the rotational dynamics of indole is slowed down by the peptide chain to which it is attached (as shown above), it is not expected to be significantly modulated by the solvent viscosity as seen with the native proteins. However, the observation of increased sensitivity of  $\phi_F$  to  $\eta$  in denatured proteins when compared to the situation in their native states indicates that covalent attachment does not completely insulate the probe from the bulk solvent. Moreover, one could associate the increased sensitivity of  $\phi_F$  to  $\eta$  in the denatured proteins to any reduced level of confinement (by nearby side chains) of the indole group in the denatured states when compared to their native states. However, the solvent accessibility inferred from KI quenching (Fig. 3) indicates a similar level of structural confinement. Hence the increased sensitivity of  $\phi_F$  to  $\eta$  in the denatured proteins is most likely the result of the absence of preferentially bound water, which could protect the indole moiety from the bulk solvent.

As mentioned in the Introduction, there is theoretical and experimental evidence indicating that the hydration layer

has 10% higher density when compared to bulk water. Does the increased density of water affect the rotational rate of probes embedded in the hydration layer? Comparison of the rates in native and denatured states of both of the proteins used in this work can be used to answer this question. The rate of the faster component of rotational diffusion ( $\phi_F$ ) was slower by 20–25% in native MBP (after normalizing the data (Table 1) to the viscosity of the medium) when compared to denatured MBP, where the water structure is largely absent, as shown by the increased sensitivity of  $\phi_F$  to bulk viscosity. However, the values of  $\phi_F$  were similar (after correction for bulk viscosity) in the case of native and denatured SC. This result would be of importance in understanding protein-ligand and protein-protein interactions. In this context it is interesting to note that the translational diffusion of protons across the membrane-water interface has been found to be very similar to that observed in bulk water (Maity and Krishnamoorthy, 1995; Kotlyar et al., 1994).

## REFERENCES

Abseher, R., H. Schreiber, and O. Steinhauser. 1996. The influence of a protein on water dynamics in its vicinity investigated by molecular dynamics simulation. *Proteins*. 25:366–378.

Afleck, R., Z.-F. Xu, V. Suzawa, K. Focht, D. S. Clark, and J. S. Dordick. 1992. Enzymatic catalysis and dynamics in low-water environments. *Proc. Natl. Acad. Sci. USA*. 89:1100–1104.

Badger, J. 1993. Multiple hydration layers in cubic insulin crystals. *Biophys. J.* 65:1656–1659.

Beveridge, D. L., S. Swaminathan, G. Ravishanker, J. M. Withka, J. Srinivasan, C. Prevost, S. Louise-May, D. R. Langley, F. M. DiCapua, and P. H. Bolton. 1993. Molecular dynamics simulation on the hydration, structure, and motions of DNA oligomers. In *Water and Biological Macromolecules*. E. Westhof, editor. CRC Press, Boca Raton, FL.

Billeter, M., P. Guntert, P. Luginbuhl, and K. Wuthrich. 1996. Hydration and DNA recognition by homeodomains. *Cell*. 85:1057–1065.

Broos, J., A. J. W. Visser, J. F. J. Engbersen, W. Verboom, A. van Hoek, and D. N. Reinoudt. 1995. Flexibility of enzymes suspended in organic solvents probed by time-resolved fluorescence anisotropy. Evidence that enzyme activity and enantioselectivity are directly related to enzyme flexibility. *J. Am. Chem. Soc.* 117:12657–12663.

Brunne, R. M., E. Liepinsh, G. Otting, K. Wuthrich, and W. F. van Gunsteren. 1993. Hydration of proteins. A comparison of experimental residence times of water molecules solvating the bovine pancreatic trypsin inhibitor with theoretical model calculations. *J. Mol. Biol.* 231: 1040–1048.

Bryant, R. G. 1996. The dynamics of water-protein interactions. *Annu. Rev. Biomol. Struct.* 25:29–53.

Burling, F. T., W. I. Weis, K. M. Flaherty, and A. T. Brunger. 1996. Direct observation of protein solvation and discrete disorder with experimental crystallographic phases. *Science*. 271:72–77.

Eftink, M. R. 1991. Fluorescence quenching: theory and applications. In *Topics in Fluorescence Spectroscopy*, Vol. 2. J. R. Lakowicz, editor. Plenum Press, New York. 53–127.

Fitter, J., R. E. Lechner, G. Buldt, and N. A. Dencher. 1996. Internal molecular motions of bacteriorhodopsin: hydration-induced flexibility studied by quasielastic incoherent neutron scattering using oriented purple membranes. *Proc. Natl. Acad. Sci. USA*. 93:7600–7605.

Fye, J. L., J. Woenckhaus, and M. F. Jarrold. 1998. Hydration of folded and unfolded gas-phase proteins: saturation of cytochrome *c* and apomyoglobin. *J. Am. Chem. Soc.* 120:1327–1328.

Gregory, R. B. 1995. *Protein-Solvent Interactions*. Marcel Dekker, New York.

Israelachvili, J., and H. Wennerstrom. 1996. Role of hydration and water structure in biological and colloidal interactions. *Nature*. 379:219–224.

Janot, J. M., A. Beeby, P. M. Bayley, and D. Phillips. 1991. The time-resolved fluorescence and anisotropy of subtilisins BPN and *Carlsberg*. *Biophys. Chem.* 41:277–287.

Jiang, J. S., and A. T. Brunger. 1994. Protein hydration observed by x-ray diffraction: solvation properties of penicillopepsin and neuraminidase crystal structures. *J. Mol. Biol.* 243:100–115.

Knapp, E. W., and I. Muegge. 1993. Heterogeneous diffusion of water at protein surfaces: application to BPTI. *J. Phys. Chem.* 97:11339–11343.

Kotlyar, A. B., N. Borovok, S. Kiryati, E. Nachliel, and M. Gutman. 1994. The dynamics of proton transfer at the C side of the mitochondrial membrane: picosecond and microsecond measurements. *Biochemistry*. 33:873–879.

Lakowicz, J. R. 1983. *Principles of Fluorescence Spectroscopy*. Plenum Press, New York.

Levitt, M., and R. Sharon. 1988. Accurate simulation of protein dynamics in solution. *Proc. Natl. Acad. Sci. USA*. 85:7557–7561.

Maity, N. C. 1997. Fluorescence dynamics in microheterogeneous media. Ph.D. thesis. University of Bombay.

Maity, H. P., and G. Krishnamoorthy. 1995. Absence of kinetic barrier for transfer of protons from aqueous to membrane-water interface. *J. Biosci.* 20:573–578.

Makarov, V. A., M. Feig, B. K. Andrews, and B. M. Pettitt. 1998. Diffusion of solvent around biomolecular solutes: a molecular dynamics simulation study. *Biophys. J.* 75:150–158.

Nandi, N., and B. Bagchi. 1997. Dielectric relaxation of biological water. *J. Phys. Chem. B*. 101:10954–10961.

Noyes, R. M. 1961. Diffusion-controlled reactions. *Prog. React. Kinet.* 1:129–160.

Partridge, J., P. R. Dennison, B. D. Moore, and P. J. Halling. 1998. Activity and mobility in low water organic media: hydration is more important than solvent dielectric. *Biochim. Biophys. Acta*. 1386:79–89.

Parsegian, V. A., R. P. Rand, and D. C. Rau. 1995. Macromolecules and water: probing with osmotic stress. *Methods Enzymol.* 259:43–94.

Phillips, G. N., and B. M. Pettitt. 1995. Structure and dynamics of the water around myoglobin. *Protein Sci.* 4:149–158.

Priev, A., A. Almagor, S. Yedgar, and B. Gavish. 1996. Glycerol decreases the volume and compressibility of protein interior. *Biochemistry*. 35: 2061–2066.

Rupley, J. A., E. Gratton, and G. Careri. 1983. Water and globular proteins. *Trends Biochem. Sci.* 8:18–22.

Sayle, R. A., and E. J. Milner-White. 1995. RASMOL: biomolecular graphics for all. *Trends Biochem. Sci.* 20:374.

Svergun, D. I., S. Richard, M. H. J. Koch, Z. Sayers, S. Kuprin, and G. Zaccai. 1998. Protein hydration in solution: experimental observation by x-ray and neutron scattering. *Proc. Natl. Acad. Sci. USA*. 95:2267–2272.

Swaminathan, R., G. Krishnamoorthy, and N. Periasamy. 1994a. Fluorescence lifetime distributions for single tryptophan proteins in the random coil state. *Biophys. J.* 67:2013–2023.

Swaminathan, R., N. Periasamy, J. B. Udgaoonkar, and G. Krishnamoorthy. 1994b. Molten globule-like conformation of barstar: a study by fluorescence dynamics. *J. Phys. Chem.* 98:9270–9278.

Swaminathan, R., U. Nath, J. B. Udgaoonkar, N. Periasamy, and G. Krishnamoorthy. 1996. Motional dynamics of a buried tryptophan reveals the presence of partially structured forms during denaturation of barstar. *Biochemistry*. 35:9150–9157.

Teeter, M. M. 1991. Water-protein interactions: theory and experiment. *Annu. Rev. Biophys. Biophys. Chem.* 20:577–600.

Timasheff, S. N., and T. Arakawa. 1996. Stabilization of protein structure by solvents. In *Protein Structure. A Practical Approach*. T. E. Creighton, editor. Oxford University Press, Oxford. 349–364.

Vanzi, F., B. Madan, and K. Sharp. 1998. Effect of protein denaturants urea and guanidinium on water structure: a structural and thermodynamic study. *J. Am. Chem. Soc.* 120:10748–10753.